Journal of Alloys and Compounds 509 (2011) 5460–5465

Contents lists available at ScienceDirect

Journal of Alloys and Compounds

journal homepage: www.elsevier.com/locate/jallcom

Neutron diffraction study of diffuse scattering in $Cu_{2-\delta}Se$ superionic compounds

S.A. Danilkin[a,*], M. Avdeev[a], T. Sakuma[b], R. Macquart[c], C.D. Ling[c]

[a] Bragg Institute, Australian Nuclear Science and Technology Organisation, Locked Bag 2001, Kirrawee DC NSW 2232, Australia, New Illawarra Road, Lucas Heights
[b] Institute of Applied Beam Science, Ibaraki University, Bunkyo 2-1-1, Mito, 310-8512, Japan
[c] School of Chemistry, The University of Sydney, Sydney, NSW 2006, Australia

ARTICLE INFO

Article history:
Received 5 August 2010
Received in revised form 18 February 2011
Accepted 20 February 2011
Available online 24 February 2011

Keywords:
Disordered systems
Semiconductors
Solid state reactions
Crystal structure
Ionic conduction
Computer simulation
Neutron diffraction

ABSTRACT

Crystal structure and short-range order in $Cu_{2-\delta}Se$ compounds were studied in superionic and non-superionic phases using high-resolution neutron diffractometer Echidna at ANSTO. In diffraction patterns of β-$Cu_{1.98}Se$ (ordered phase at ambient T), both Bragg peaks and diffuse background change sharply through the $\beta \rightarrow \alpha$ structural phase transition at $T = 414$ K during heating. In case of α-$Cu_{1.75}Se$ (disordered superionic phase at ambient T) the changes are monotonic, showing gradual shifts of Bragg peaks and increased intensity of the diffuse background as a function of temperature. On cooling, both compounds undergo a $\beta \rightarrow \beta'$ transformation. Diffuse scattering in the α-phase shows an oscillating dependence on wavevector, with broad peaks centred at $Q \sim 3$, 5.5 and 8 Å^{-1}. The measurements taken in energy dispersive mode show that the oscillating diffuse background arises from correlated thermal displacements of the ions. Diffuse scattering is higher for compositions close to stoichiometry and increases with temperature. Theoretical calculations show that the increase in diffuse intensity both with temperature and Cu content is related to correlated thermal vibrations of Se and Cu atoms, with Se–Cu(*8c*, *32f*) and Cu(*8c*)–Cu(*8c*) correlations being the most important.

1. Introduction

The compound $Cu_{2-\delta}Se$ ($0 \le \delta \le 0.25$) is a mixed ionic-electronic conductor. For stoichiometric Cu_2Se the phase transition temperature to the cubic superionic α-phase is 414 K, but the transition temperature depends on the composition and decreases with increasing δ [1]. Over the concentration range of $\delta = 0.15$–0.25 the superionic α-phase exists at room temperature. In cooling from the superionic α-phase transforms into single β-phase for $\delta < 0.05$. In the range $\delta = 0.05$–0.25, cooling results in eutectoid decomposition to a mixture of the α-phase and Cu_3Se_2 [1]. Another order–disorder $\beta \rightarrow \beta'$ transition occurs at $T \approx 150$ K. Ionic conductivity of α-Cu_2Se is about 2 S/cm at 600 K and decreases gradually with deviation from stoichiometry, vanishing at the boundary of the homogeneity region at $\delta \approx 0.25$ [2]. According to [1,2] only a fraction of Cu atoms takes part in the ionic transport: the number of mobile atoms is about 1/3–1/8 of the total cation concentration in stoichiometric Cu_2Se and decreases with increasing δ causing the ionic conductivity to drop.

The structures of both α- and β-phases are of antifluorite-type with Se atoms in face-centred cubic (fcc) positions and Cu atoms distributed over the large number of tetrahedral (*8c*), trigonal (*32f*) and octahedral (*4b*) sites, many of which are vacant. In the low-temperature β-$Cu_{2-\delta}Se$ phase the Cu cations form an ordered structure in large distorted unit cell. A review of the structural models can be found in papers [3–6] and references therein, but the crystal structure of β-phase is not conclusively established from the diffraction data. The high temperature α-phase is considered to have randomly distributed Cu ions over interstitial sites; however, information about the fractions of Cu in different interstitial positions is controversial [6–12]. For instance, in the split-site model of Heyding and Murray [7] Cu ions are located in tetrahedral *8c* (1/4, 1/4, 1/4) positions and the remaining Cu cations are in trigonal *32f* (*xxx*) ($x = 0.33$) sites. Similar results were recently reported by Skomorokhov et al. [8]. Sakuma [9] suggests that Cu is in trigonal $32f_1$ ($x = 0.297$) and $32f_2$ ($x = 0.471$) sites. In single crystal X-ray study Yamamoto and Kashida [6] found that the split-site model with most of Cu atoms located in tetrahedral and trigonal sites and small fraction of Cu atoms in octahedral *4b* (1/2, 1/2, 1/2) sites had the same order of *R*-factor as the anharmonic model for the atoms located mainly in the tetrahedral sites. In the anharmonic model 95% of the Cu atoms are in the tetrahedral sites with small fraction in the octahedral positions. The Fourier map of the average structure of α-Cu_2Se at 160 °C shows that the electron density of the Cu atoms has a long tail toward the octahedral site [10]. Similar

* Corresponding author at: Bragg Institute, Australian Nuclear Science and Technology Organisation, Locked Bag 2001, Kirrawee DC NSW 2232, Australia.
Tel.: +61 2 9717 3338; fax: +61 2 9717 3606.
E-mail address: s.danilkin@ansto.gov.au (S.A. Danilkin).

0925-8388/$ – see front matter © 2011 Elsevier B.V. All rights reserved.
doi:10.1016/j.jallcom.2011.02.101

results were obtained in another single crystal study by Oliveria et al. [11].

Disordered distribution of Cu atoms gives rise to broad diffuse maxima observed in neutron diffraction patterns of polycrystalline and single crystal samples of copper selenide [9,13–15]. The diffuse background generally contains the elastic and inelastic scattering components originating from the static disorder and dynamic correlations, both of which affect ionic conductivity [13–15]. It is therefore of interest to study structural modifications along with the intensity and Q-dependence of diffuse scattering in Cu–Se compounds, as a function of temperature and composition to explore different types of disorder and short range correlations.

We studied structural modifications in $Cu_{1.75}Se$ and $Cu_{1.98}Se$ compounds in the temperature range 4–430 K. Between these temperature points $Cu_{1.75}Se$ undergoes the eutectoid and superstructural $\beta \rightarrow \beta'$ transformations:

$$\alpha \overset{\sim 290\,K}{\rightarrow} \beta + Cu_3Se_2 \overset{\sim 150\,K}{\rightarrow} \beta' + Cu_3Se_2$$

According to Korzhuev et al. [1] the amount of Cu_3Se_2 phase depends on cooling rate and can be suppressed by "fast" cooling to liquid nitrogen temperature.

The $Cu_{1.98}Se$ compound transforms via the following series of transitions:

$$\alpha \overset{414\,K}{\rightarrow} \alpha + \beta \overset{\sim 350\,K}{\rightarrow} \beta \overset{\sim 150\,K}{\rightarrow} \beta'$$

The paper is divided into 5 sections. Section 2 provides the experimental details of the measurements. In Section 3 we present the experimental results and discuss crystal structure evolution for $Cu_{1.75}Se$ and $Cu_{1.98}Se$ during heating from the ambient temperature to 430 K and on cooling to 4 K. Section 4 deals with refinement of the structural model, calculations of diffuse scattering and discussion, followed by conclusions.

2. Experimental details

The $Cu_{2-\delta}Se$ samples were synthesised using the method outlined by Kashida and Akai for Cu_2Se [3]. Stoichiometric quantities of Cu ($\delta = 0.02$ and 0.23) (Umicore, 2×10 mm rods, 99.99%) and Se (Aldrich, 2 mm pellets ground up, 99.999+%) were placed in quartz tubes (9.6 mm outer and 7.0 mm inner diameter) which were then sealed under vacuum using a hydrogen oxygen torch. The resulting ampoules were rested on alumina boats at an angle of approximately 30° and then heated in a muffle furnace from room temperature to 1000 °C at a rate of 20 °C/min and kept at 1000 °C for seven days before cooling at a rate of 1 °C/min down to room temperature. The resulting compounds were a shiny black mass of uniform appearance filling approximately two thirds of the volume of the quartz ampoules.

We used two samples of $Cu_{2-\delta}Se$ with nominal composition of Cu/Se = 1.77 prepared in two separate runs for low and elevated temperature measurements. X-ray and neutron diffraction of these samples show that both of them are pure α-phase at ambient temperature. The lattice parameters of the two samples determined using neutron diffraction data are very close to each other ($a = 5.7411(2)$ Å and 5.7494(3) Å) and to the values determined from X-ray data. According to the published composition dependence of the lattice parameter [12,16], this corresponds to composition Cu/Se = 1.75. For $Cu_{1.98}Se$ we performed DSC measurement to determine $\beta \rightarrow \alpha$ transition temperature and verify the sample composition. The onset and completion temperatures of $\beta \rightarrow \alpha$ phase transition in the $Cu_{1.98}Se$ sample were estimated as 360 K and 410 K. The thermoanalytical curves of $Cu_{1.98}Se$ on heating and cooling were very close to the literature data [17] for a composition of 1.99, which is in turn very close to the nominal composition of our sample.

Neutron powder diffraction data were collected with the Echidna neutron diffractometer at OPAL reactor, ANSTO [18]. Echidna is high-resolution multidetector powder diffractometer optimised for structure determination of new materials. The data were collected at wavelengths $\lambda = 1.300$ Å or $\lambda = 1.622$ for the $Cu_{1.75}Se$ and $Cu_{1.98}Se$ samples loaded in cylindrical vanadium containers. For the experiments at or above room temperature we used a standard cryofurnace, and for low temperature experiments we used a liquid helium cryostat. Diffraction patterns were taken at fixed temperatures of 360 K and 430 K on heating from 300 K. On cooling to temperature of 4 K we used two regimes. In the "fast" cooling mode the sample was cooled to ~150 K at rate of ~10 K/min and at ~2 K/min below this temperature. In the "slow" cooling regime the cooling rate was ~1 K/min and data were collected during ramping from 300 K to set points of 244 K, 202 K 133 K 50 K and 4 K. The diffraction patterns were corrected for the data for an empty sample container collected in the same conditions.

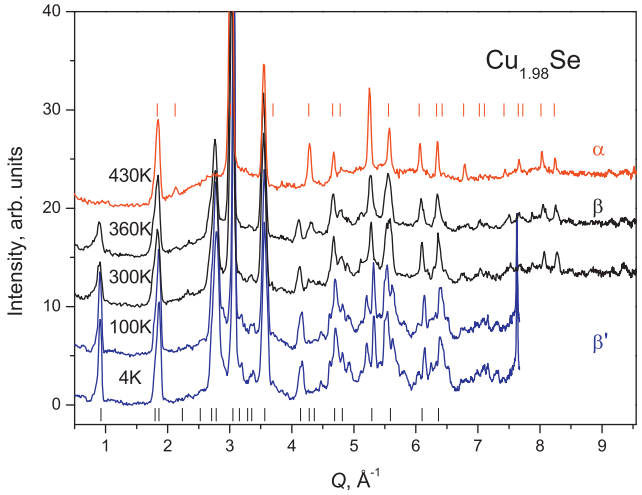

Fig. 1. Diffraction patterns of $Cu_{1.98}Se$ at different temperatures. Measurements were taken at wavelength $\lambda = 1.300$ Å on heating from $T = 300$ to 430 K; and at $\lambda = 1.662$ Å on cooling from $T = 300$ K to 4 K. Top tick marks correspond to peak positions in α-$Cu_{1.98}Se$ at 430 K (Table 1); bottom tick marks show peak positions of β-$Cu_{1.98}Se$ from reference [19].

3. Experimental results

3.1. $Cu_{1.98}Se$

On heating the diffraction patterns of $Cu_{1.98}Se$ were taken at temperatures of 360 K and 430 K starting from 300 K (Fig. 1). Spectra of β-$Cu_{1.98}Se$ at 300 and 360 K are consistent with data of De Montreuil for bellidoite [19]. At 430 K $Cu_{1.98}Se$ is in superionic α-phase. The pronounced change is observed between diffraction patterns of β-$Cu_{1.98}Se$ taken at 360 K just below the $(\alpha + \beta)$ region and in superionic α-phase at 430 K. This phase transformation is related to disruption of ordered superstructure in a Cu sublattice and transition from distorted cubic to anti-fluorite structure [4–6,10] and manifests itself in disappearing of the large number of small reflections corresponding to ordered β-phase (Fig. 1). Disordering of Cu atoms shows itself also as smoothing and increasing intensity of broad peaks of diffuse scattering centred at $Q \sim 3$, 5.5 and 8 Å^{-1}.

On cooling from 300 K modifications are seen between diffraction patterns at 300 K and 100 K reflecting the superstructural $\beta \rightarrow \beta'$ transition at $T \approx 150$ K [1,21]. At the same time spectra at 100 K and 4 K show very little difference apart from the change in peak positions with temperature.

3.2. $Cu_{1.75}Se$

The diffraction patterns of $Cu_{1.75}Se$ were collected on heating at temperatures 360 K, 430 K starting from 300 K. Data taken at 300, 360 and 430 K (Fig. 2) show the Bragg peaks corresponding to the α-phase and broad diffuse features at $Q \sim 3$, 5.5 and 8 Å^{-1} similar to $Cu_{1.98}Se$ at 430 K (Fig. 1). The intensity of the diffuse peaks increases continuously with temperature. The difference in intensity is more pronounced at lower Q: the amplitude of the first diffuse maximum at $Q \sim 3$ A^{-1} at 430 K is about 20% higher than at 300 K, while the peak at $Q > 7.5$ A^{-1} demonstrates only slight increase.

As noted above the $\alpha \rightarrow \beta$ phase transformation of $Cu_{2-\delta}Se$ compounds with $\delta > 0.05$ is of an eutectoid type that results in complex hysteretic temperature dependencies of electrophysical properties and phase compositions [1]. Therefore the measurements of the structural modifications on cooling were performed in two regimes. In the "fast" cooling regime we were trying to quench the α-phase at 4 K in order to see modifications of vibrational components in diffuse scattering due to the temperature.

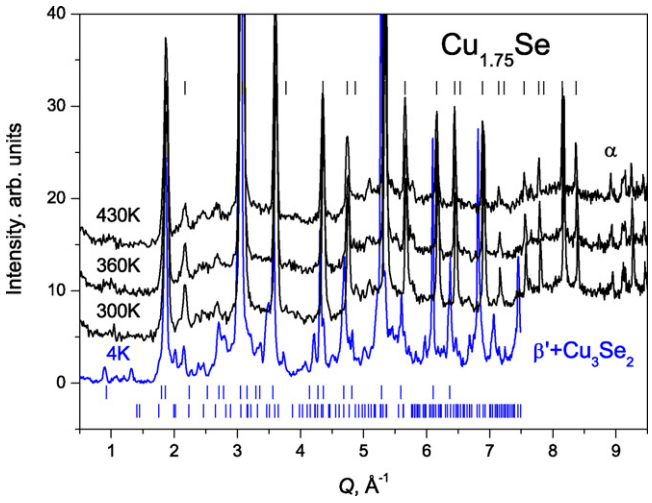

Fig. 2. Diffraction patterns of $Cu_{1.75}Se$ at different temperatures. Measurements were taken at wavelength $\lambda = 1.300$ Å on heating from $T = 300$ to 430 K; and at $\lambda = 1.662$ Å after "fast" cooling from $T = 300$ K to 4 K. Top tick marks indicate the peak positions in α-$Cu_{1.75}Se$ at 430 K (Table 1); middle tick marks show peak positions of β-$Cu_{1.98}Se$ from reference [19]; bottom tick marks correspond to Cu_3Se_2 from reference [20].

The diffraction pattern of $Cu_{1.75}Se$ sample at 4 K after "fast" cooling shows the presence of small amounts of the β′ and Cu_3Se_2 phases in addition to the α-phase. This indicates that cooling was not fast enough to quench the α-phase. Peak positions of Cu_3Se_2 shown in Fig. 2 correspond to data of Milman for Umangite from the reference [20]. At the same time, a considerable reduction in the intensity of the broad diffuse component (about 50% in amplitude for the first and the second diffuse peaks) is clearly seen. This relates to a decrease in the mean square amplitude of atomic vibrations with temperature, accounting for the intensity of the thermal/vibration diffuse component.

Distinctive structural modifications were observed during "slow" cooling of $Cu_{1.75}Se$ sample from 300 to 4 K. The patterns taken on cooling at temperatures above ~200 K show only small changes and correspond to the α-phase (see Fig. 1 in Supplement). In the temperature range 200–130 K the peaks from the Cu_3Se_2 phase appear and no further changes occur at temperatures below 130 K. These changes in structure are in general agreement with the $\alpha \rightarrow \beta$ and $\beta \rightarrow \beta'$ phase transformations at ~290 and ~150 K reported previously [1,21]. Note that amount of Cu_3Se_2 phase is substantially higher in the "slow" cooled sample than in the "quenched" one.

4. Discussion

4.1. Average crystal structure of α-phase

The high temperature phase is considered to have randomly distributed Cu ions over interstitial sites, but information about the location of Cu in the lattice is controversial in spite of a large body of research [7–12]. As already noted, the anti-fluorite structure of α-$Cu_{2-\delta}Se$ compounds has a number of tetrahedral (*8c*), octahedral (*4b*) and trigonal (*32f*) interstitial positions available to Cu atoms and most of them are vacant. The key issue concerns the fractions of Cu atoms in different interstitial sites, and because the Cu atoms are highly mobile and delocalised the standard analysis of the average structure suffers from strong correlations between parameters, particularly the positional parameters and vibrational/thermal displacements.

In the present study the distribution of Cu atoms over crystallographic positions has been analysed by Rietveld method using the GSAS software [22]. Different split-site models were tested assuming the overall *Fm*3*m* symmetry. During analysis, the total content of Cu atoms was fixed to the nominal composition. We found that the model with occupation of both *8c* and *32f* ($x = 0.39/0.41$) sites gives better agreement with experiment for $Cu_{1.75}Se$ and $Cu_{1.98}Se$ compared to the model with only *8c* site occupied (Table 1). Our results are in general agreement with previous X-rays studies [6–8] showing that Cu atoms predominantly occupy the *8c* and *32f* sites. We did not find statistically significant improvement of refinement quality when allowing Cu atoms occupy the *4b* position. This is in contradiction with the results of Yamamoto and Kashida obtained using X-ray single crystal diffraction and the maximum entropy method [10]. They found that the Cu ions have a noticeable population of the octahedral *4b* positions in addition to *8c* at elevated temperature in the α-phase.

4.2. Diffuse scattering

In addition to Bragg peaks, diffraction patterns of the $Cu_{2-\delta}Se$ compounds have broad peaks of diffuse scattering centred at $Q \sim 3$, 5.5 and 8 $Å^{-1}$. The first two maxima were previously observed in neutron diffraction patterns of polycrystalline samples of copper selenide [13,15] and in anomalous X-ray scattering experiment [9]. The first diffuse peak at $Q \sim 3$ $Å^{-1}$ was also clearly seen in our X-ray diffraction measurement with Co radiation during the characterisation of samples.

The positions of diffuse maxima in $Cu_{1.75}Se$ and $Cu_{1.98}Se$ are close to each other, but intensity varies differently with temperature. In α-$Cu_{1.75}Se$ the intensity of the diffuse peaks increases slightly in the temperature range 300–430 K (Fig. 2). This effect is more pronounced for the first peak at $Q \sim 3$ $Å^{-1}$ and tends to diminish with Q (see Fig. 2 in Supplement). In $Cu_{1.98}Se$ the Bragg reflections and intensity and shape of broad peaks change sharply through the $\beta \rightarrow \alpha$ phase transition (Fig. 1). At 300 K and 360 K in the low-temperature β-phase, these broad peaks are almost identical and probably arise from numerous overlapped Bragg peaks of a large supercell. At 430 K in α-$Cu_{1.98}Se$, the peaks are smoothed-out and have overall shape similar to those of α-$Cu_{1.75}Se$. The intensities of the diffuse peaks in α-$Cu_{1.98}Se$ is higher, particularly the first diffuse peak which is about 30% higher in intensity than in $Cu_{1.75}Se$ (Fig. 3 in Supplement).

The diffuse background generally contains both elastic and inelastic scattering components which originate from the static disorder and dynamic correlations. Contributions from static and thermal distortions/correlations to scattering intensity cannot be

Table 1
The Cu atom distribution over crystallographic sites in $Cu_{1.75}Se$ and $Cu_{1.98}Se$ in α-phase.

Composition	T (K)	$n_{Cu(8c)}$	$n_{Cu(32f)}$	x	B (Cu)	B (Se)	a (Å)	R_p (χ^2)
$Cu_{1.75}Se$	430	0.71(2)	0.046(2)	0.403(2)	4.2(1)	2.6(1)	5.7598(3)	5.7/2.3
$Cu_{1.75}Se$	300	0.78(1)	0.030(2)	0.410(2)	2.9(1)	1.9(1)	5.7411(2)	5.5/2.1
$Cu_{1.98}Se$	430	0.73(2)	0.068(2)	0.390(2)	7.1(1)	3.6(1)	5.8426(7)	4.3/2.7

T – temperature; $n_{Cu(8c)}$ and $n_{Cu(32f)}$ – occupancies of *8c* and *32f* (x,x,x) sites; x – Cu positional parameter; B (Cu) and B (Se) – isotropic displacement parameters of Cu and Se atoms; a – lattice parameter; R_p (χ^2) – Reitveld refinement quality factors.

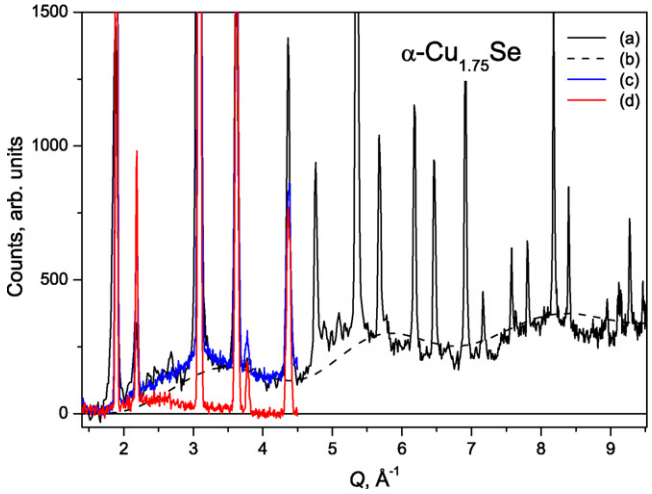

Fig. 3. Diffraction patterns of $Cu_{1.75}Se$ at $T = 300$ K. (a) Experiment (Echidna); (b) diffuse scattering, calculations; Experiment (E1) [15]: (c) 2-axis mode; (d) 3-axis (elastic window) mode.

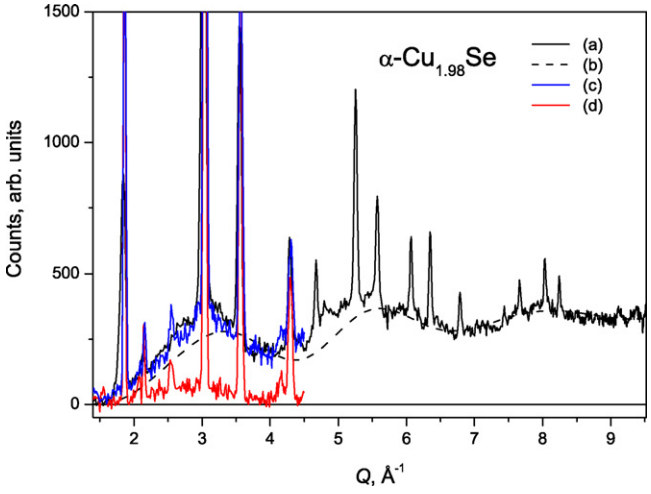

Fig. 4. Diffraction patterns of $Cu_{1.98}Se$ at $T = 430$ K. (a) Experiment (Echidna); (b) diffuse scattering, calculations; Experiment (E1) [15]: (c) 2-axis mode; (d) 3-axis (elastic window) mode.

distinguished in the present non-energy dispersive diffraction experiment. For this reason a comparison of the current data with our previous results on $Cu_{1.75}Se$ and $Cu_{1.98}Se$ samples performed using triple-axis spectrometer in so called "elastic window method" is important [15]. Contrary to a conventional diffraction experiment, in this method neutrons scattered by a sample are filtered by an analyser crystal before reaching the detector. The analyser crystal reflects only (within the instrument resolution) the scattering processes with zero energy transfer, which correspond to elastic scattering. As a result the thermal/inelastic contributions to the scattering intensity are filtered out.

Our previous measurements for $Cu_{1.75}Se$ and $Cu_{1.98}Se$ samples with the triple-axis spectrometer E1 were performed at a neutron wavelength of 2.42 Å [15]. The diffraction patterns were collected both with and without the analyser crystal after sample, using otherwise identical experimental conditions and were normalised to each other taking into account the sample mass, monitor counts and intensity of the Bragg reflections [15]. In order to compare these data with the diffraction patterns measured with Echidna diffractometer, the spectra taken in non-dispersive mode with E1 spectrometer were normalised to the intensity of the maximum at 3 $Å^{-1}$ of corresponding spectra from Echidna diffractometer.

Fig. 3 shows diffraction patterns of β-$Cu_{1.75}Se$ measured on Echidna and E1 at 300 K. It can be seen that spectra from E1 taken in conventional 2-axis mode agree well with diffraction pattern from Echidna. In contrast, data taken in an energy-dispersive "elastic window" mode show strong suppression of diffuse intensity. Similarly, the diffuse background is suppressed in α-$Cu_{1.98}Se$ at 430 K (Fig. 4), while the diffraction pattern taken without the analyser is practically identical to the Echidna data. This indicates strong contributions from inelastic scattering to the diffuse scattering related to dynamic correlations of thermal/vibrational displacements in the superionic phase. The dynamic origin of short range correlations among the mobile ions in $Cu_{1.8}Se$ was also mentioned in paper [14].

On the other hand, the diffraction pattern of non-superionic β-$Cu_{1.98}Se$ at 300 K shows a less pronounced difference between patterns measured with and without the analyser crystal (Fig. 5). Only ~50% of the peak intensity at 3 $Å^{-1}$ is filtered out in β-$Cu_{1.98}Se$ at 300 K in comparison to 80–90% reduction in the peak intensity observed in α-$Cu_{1.75}Se$ at 300 K and α-$Cu_{1.98}Se$ at 430 K.

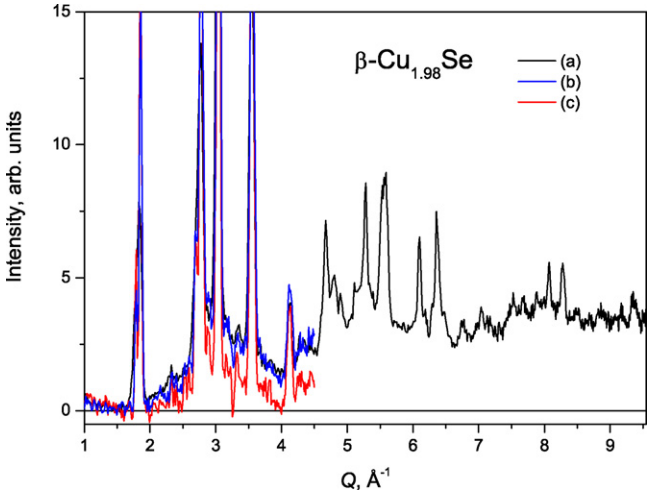

Fig. 5. Diffraction patterns of $Cu_{1.98}Se$ at $T = 300$ K. (a) Experiment (Echidna); Experiment (E1) [15]: (b) 2-axis mode; (c) 3-axis (elastic window) mode.

4.3. Calculations of diffuse scattering

4.3.1. Theoretical model

The theoretical model used in calculations takes into account both static and dynamic correlations in disordered compounds. According to [9,13] the diffuse intensity including the term related to thermal displacements of atoms is expressed as follows:

$$I_D = N_0 \sum_i b_i b_i^* (1 - p_i \exp(-2M_i)) + N_0 \sum_{i,j}^{i \neq j} \sum_{s'(j)} b_i b_j \{\alpha_{r_{s(i)s'(j)}} [\exp(-(M_i + M_j)(1 - \lambda_{r_{s(i)s'(j)}})) - \exp(-(M_i + M_j))] + (1 - p_i)(\alpha_{r_{s(i)s'(j)}} - \beta_{r_{s(i)s'(j)}}) \exp(-(M_i + M_j))\} Z_{r_{s(i)s'(j)}} S_{r_{s(i)s'(j)}} \quad (1)$$

where N_0 is the number of unit cells per unit volume; b_i is the neutron scattering length; p_i is the probability of finding an atom i in any site s; M_i is the Debye–Waller factor of an atom i; $Z_{r_{s(i)s'(j)}}$ is the number of sites at a distance r around an atom i occupied by an atom j; $S_r = sin(Qr)/Qr$, r is the distance between sites $s(i)$ and $s(j)$. The parameters α and β relate to static correlations: α_r gives the probability of finding an atom at distance r from the occupied site and

β_r is the probability of finding an atom at a distance r from a vacant site. Correlation parameters between thermal displacements λ_r are given by:

$$\lambda_{r_{s(i)s'(j)}} = \frac{2\langle \Delta r_{s(i)} \Delta r_{s'(j)} \rangle}{\langle (\Delta r_{s(i)})^2 \rangle + \langle (\Delta r_{s'(j)})^2 \rangle} \quad (2)$$

where Δr_s is the displacement caused by thermal vibrations.

Calculations of diffuse scattering were performed assuming occupation of *8c* and *32f* sites by Cu. For different compositions and temperature, the occupancy parameters, atomic displacement parameters and lattice parameters were taken from the structural refinement (Table 1). The static correlations between Cu atoms were taken into account at distances $r \leq 3.0$ Å using two sets of parameters for distances below and above $r = 2.3$ Å. The correlations between thermal vibrations of Se–Cu and Cu–Cu atoms were considered at distances $2.3 < r \leq 4.0$ Å and were described by 2 parameters depending on distance between atoms. The parameters of thermal correlations remained fixed for all samples and temperatures. Correlations between Se atoms were not included due to the larger interatomic distance. The characteristic set of parameters used in simulations of diffuse scattering is given in Table 2 for α-$Cu_{1.75}Se$ at 430 K.

4.3.2. Results and discussion

The oscillating structure of diffuse background arises from correlations of thermal vibrations (Eq. (1)). First we considered the thermal correlations only between Se and Cu atoms. We found that the calculated diffuse scattering consists of 3 broad peaks in agreement with experiment, but positions of first and second diffuse peaks were at higher Q values than in experiment. Agreement with experiment improved considerably after taking into account the correlations between Cu atoms.

Figs. 3, 4 and 6 show calculated diffuse intensity of α-$Cu_{1.75}Se$ and α-$Cu_{1.98}Se$ at 300 and 430 K. Calculated curves were normalised to experimental data in the Q range 7.5–9.5 $Å^{-1}$ after subtraction of constant component in the same manner as for the experimental data. It can be seen that the intensity of the diffuse scattering increases with temperature and is higher in the $Cu_{1.98}Se$ compound. Changes in first two peaks at $Q \sim 3$ and 5.5 $Å^{-1}$ are more pronounced. This is apparent from comparison of the diffuse backgrounds in $Cu_{1.75}Se$ at different temperatures (Fig. 2 in Supplement) and $Cu_{1.75}Se$ and $Cu_{1.98}Se$ at 430 K (Fig. 3 in Supplement). Note that the increase in the intensity of diffuse scattering correlates with concentration and temperature dependences of ionic conductivity, which is higher at compositions close to stoichiometry and increase with temperature [1,2]. As shown below, this is mostly related to contributions from Se–Cu and Cu–Cu thermal correlations.

Table 2
Static and thermal correlation parameters between Se and Cu atoms in $Cu_{1.75}Se$ at 430 K.

	r (Å)	λ_r	$(\alpha-\beta)_{i,j}$
i, j = *8c*, *32f*	<2.3	–	$-p_j/(1-p_i)$
i, j = *8c*, *8c*	$2.3 < r \leq 3.0$	0.7	−0.086
i, j = *8c*, *32f*	$2.3 < r \leq 3.0$	0.7	0.008
i, j = *32f*, *8c*	$2.3 < r \leq 3.0$	0.7	0.064
i, j = *32*, *32f*	$2.3 < r \leq 3.0$	0.7	0
i, j = *8c*, *32f*	$3.0 < r \leq 4.0$	0.4	0
i, j = *8c*, *8c*	>4	0	0
i, j = *8c*, *32f*	>4	0	0
i, j = *32f*, *8c*	>4	0	0
i, j = *32*, *32f*	>4	0	0
i, j = Se, *32f*	$2.3 < r \leq 3.0$	0.7	–
i, j = Se, *8c*	$2.3 < r \leq 3.0$	0.7	–
i, j = Se, *32f*	$3.0 < r \leq 4.0$	0.4	–
i, j = Se, *8c*	$3.0 < r \leq 4.0$	0.4	–
Se–Se		0	–

r is the coordination shell; λ_r is the correlation among the thermal displacements of atoms; $(\alpha-\beta)_{i,j}$ is the static correlation probability function; *8c* and *32f* are the atomic positions of cations. Probabilities p_{8c} and p_{32f} are equal to 0.71 and 0.046, respectively.

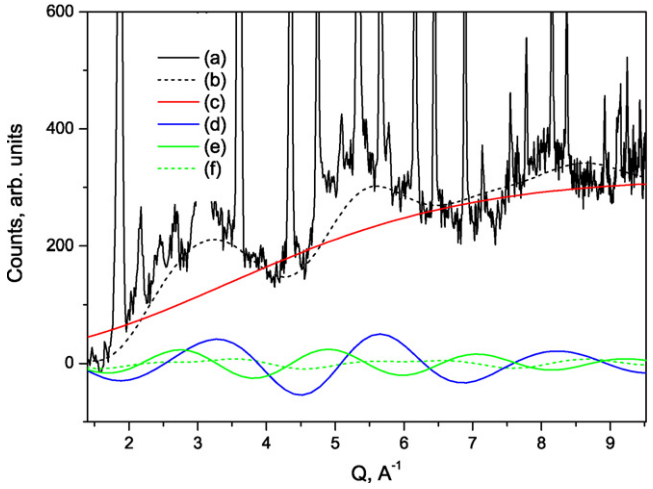

Fig. 6. Contributions to diffuse scattering in $Cu_{1.75}Se$ at $T = 430$ K. (a) Experiment (Echidna); (b) calculated diffuse scattering (total + incoherent); (c) thermal diffuse, uncorrelated; (d) thermal diffuse, Se ↔ Cu(*8c*, *32f*) correlations; (e) thermal diffuse, Cu(*8c*) ↔ Cu(*8c*) orrelations; (f) thermal diffuse, Cu(*8c*) ↔ Cu(*32f*) correlations.

In addition to total diffuse scattering Fig. 6 shows contributions from the static and thermal correlations separately. In our model the thermal contributions from anion–anion and cation–cation $s = s'$ pairs were calculated in the Einstein approximation without correlation. As a result we obtain relatively strong contributions which smoothly increase with Q. Contributions from static correlations are much lower in magnitude, have a wide maximum at $Q \sim 3$ $Å^{-1}$ and disappear gradually with increasing Q (Fig. 4 in Supplement). The oscillating contributions originate from Se–Cu and Cu–Cu thermal correlations. The major contributions are from Se–Cu(*8c*, *32f*) and Cu(*8c*)–Cu(*8c*) correlations (Fig. 6). The diffuse scattering arising from Cu(*8c*)–Cu(*32f*) correlations is also relatively strong and comparable with contribution from Se–Cu(*32f*) (Fig. 4 in Supplement). The contribution to diffuse scattering from Cu(*32f*)–Cu(*32f*) correlations is noticeably lower than from other Cu–Cu correlations. The correlation parameter λ_r (Table 1) has rather large positive value that corresponds to strong correlation in thermal motions which occur in the same direction (a value of zero corresponds to random displacements).

The relatively strong contributions arising from Se–Cu(*32f*) and Cu(*8c*)–Cu(*32f*) thermal correlations are essential for the overall agreement of the calculations with experimentally observed diffuse scattering. This fact also provides support for our crystallographic model with occupation of both *8c* and *32f* sites. Furthermore, the occupation of *32f* sites by Cu atoms in the average structural model is consistent with elongation of the electron density of the Cu atoms toward the octahedral site previously reported based on X-ray diffraction data [10,11]. In other words, occupation of the 32f sites can take place due to migration of Cu ions along ⟨1 1 1⟩ direction from *8c* toward octahedral *4b* position. However according to the recent quasi-elastic neutron scattering study of diffusion in α-$Cu_{2-\delta}Se$ [23] the *4b* sites are not in the diffusion path; the Cu atoms most probably diffuse between the nearest *8c* sites through the *32f* sites along the periphery of the octahedral hole.

5. Conclusions

Crystal structure and short-range order in $Cu_{2-\delta}Se$ compounds were studied in superionic and non-superionic phases using neutron diffraction. The behaviour of $Cu_{1.98}Se$ and $Cu_{1.75}Se$ on heating from ambient temperature is distinctly different. In $Cu_{1.98}Se$ the diffraction patterns show sharp changes in the structure of Bragg peaks and diffuse background during $\beta \rightarrow \alpha$ phase transition, while in case of α-$Cu_{1.75}Se$ the changes are monotonic showing a gradual shift of Bragg peaks and increase in intensity of diffuse background as a function of temperature. On cooling both compounds undergo $\beta \rightarrow \beta'$ transformations in agreement with the previous data.

In the superionic α-phase both $Cu_{1.75}Se$ and $Cu_{1.98}Se$ show broad peaks of diffuse scattering centred at $Q \sim 3$, 5.5 and 8 $Å^{-1}$. Data taken in energy dispersive mode show that the oscillating diffuse background arises from inelastic scattering associated with correlated thermal displacements of the ions. The intensity of the diffuse scattering changes with temperature and composition, being higher for the compositions close to stoichiometry and increases with temperature. These trends are in agreement with the data on ionic conductivity [1,2].

Theoretical calculations show that the increase in diffuse intensity both with temperature and increasing Cu content is related to contributions from correlated thermal vibrations of Se and Cu atoms, with Se–Cu(*8c*, *32f*) and Cu(*8c*)–Cu(*8c*) correlations being most important.

Acknowledgements

This work was supported by the Australian Research Council – Discovery Projects (DP0984525). The authors would like to thank R. Russell for the DSC measurements of the samples studied in this work.

Appendix A. Supplementary data

Supplementary data associated with this article can be found, in the online version, at doi:10.1016/j.jallcom.2011.02.101.

References

[1] M.A. Korzhuev, V.F. Bankina, B.F. Gruznov, G.S. Bushmarina, Sov. Phys. Semiconduct. 23 (1989) 959–962.
[2] R.A. Yakshibaev, V.N. Konev, M.K. Balapanov, Sov. Phys. Solid State 26 (1984) 2189–2191.
[3] S. Kashida, J. Akai, J. Phys. C: Solid State Phys. 21 (1988) 5329–5336.
[4] O. Milat, Z. Vučić, B. Ruščić, Solid State Ionics 23 (1987) 37–47.
[5] N. Frangis, C. Manolikas, S. Amelinckx, Phys. Status Solidi A126 (1991) 9–22.
[6] K. Yamamoto, S. Kashida, J. Solid State Chem. 93 (1991) 202–211.
[7] R.D. Heyding, R.M. Murray, Can. J. Chem. 54 (1976) 841–848.
[8] A.N. Skomorokhov, D.M. Trots, M. Knapp, N.N. Bickulova, H. Fuess, J. Alloys Compd. 421 (2006) 64–71.
[9] T. Sakuma, Bull. Electrochem. 11 (1995) 57–80.
[10] K. Yamamoto, S. Kashida, Solid State Ionics 48 (1991) 241–248.
[11] M. Oliveria, R.K. McMullan, B.J. Wuensch, Solid State Ionics 28–30 (1988) 1332–1337.
[12] N.N Bickulova, S.A. Danilkin, H. Fuess, E.L. Yadrovski, A.I. Beskrovni, A.N. Skomorokhov, Z.A. Yagafarova, G.N. Asylguzhina, Crystallogr. Rep. 48 (2003) 370–373.
[13] T. Sakuma, T. Aoyama, H. Takahashi, Y. Shimojo, Y. Morii, Phys. B 213–214 (1995) 399–401.
[14] R.J. Cava, N. Hessel Andersen, K. Clausen, Solid State Ionics 18–19 (1986) 1184–1187.
[15] S.A. Danilkin, J. Alloys Compd. 467 (2009) 509–513.
[16] A. Tonejc, J. Mater. Sci. 15 (1980) 3090–3094.
[17] K. Chrissafis, K.M. Paraskevopoulos, C. Manolikas, J. Therm. Anal. Calorim. 84 (2006) 195–199.
[18] K.-D. Liss, B.A. Hunter, M.E. Hagen, T.J. Noakes, S.J. Kennedy, Phys. B 385–386 (2006) 1010–1012.
[19] L. De Montreuil, Econ. Geol. 70 (1975) 384–387.
[20] V. Milman, Acta Crystallographica B 58 (2002) 437–447.
[21] T Ohtani, Y. Tachibana, J. Ogura, T. Miyake, Y. Okada, Y. Yokota, J. Alloys Compd 279 (1998) 136–141.
[22] A.C. Larson and R.B. Von Dreele, General structure analysis system (GSAS), Los Alamos National Laboratory Report LAUR 86–748 (2000); B.H. Toby, EXPGUI, a graphical user interface for GSAS, J. Appl. Cryst. 34 (2001) 210–213.
[23] S.A. Danilkin, M. Avdeev, T. Sakuma, R. Macquart, C.D. Ling, M. Rusina, Z. Izaola, Ionics 17 (2010) 75–80.